doi:10.36487/ACG_repo/2435_B-03
9th International Conference and Exhibition on Mass Mining, Kiruna Sweden 17-19 September 2024

# Development of the geotechnical model for the Jwaneng underground project

**M. J. Dunn and L. Q. Kebatsetse**
*Debswana Diamond Company, Botswana*

## ABSTRACT

The Debswana Diamond Company (DDC) Jwaneng Mine in Botswana, is a large open pit diamond mine extracting three kimberlite pipes. Open pit operations will cease in the early 2030's; studies are being undertaken to transition to an underground operation by the time open pit mining ceases. It is anticipated that underground mining will be undertaken using a combination of sublevel retreat (SLR), sublevel caving (SLC) and block caving (BC) methods; mining will extend to a depth of ~1000 m below surface.

The Jwaneng open pit has been in full production since 1982 and has a mature high-quality geotechnical model that has been progressively developed and improved over many years. Debswana makes use of a Geotechnical Review Board to guide the development of the geotechnical model. The geotechnical model comprises of several components: lithology model, major structures model, rock mass model, fabric model, hydrogeology model and stress field model. The geotechnical model is based on a significant amount of data (>226 km of logged core and >13,000 laboratory tests) and various components of the geotechnical model are regularly updated; generally, this is planned to coincide with the study stage, the intent being to meet the confidence level required for each stage.

Understanding the in-situ stress regime is an important input for underground mine design and has a significant impact on design analyses including numerical modelling. Various evaluations have been undertaken and this includes stress measurements using the Sigra In-situ Stress Test (IST) and the Deformation Rate Analysis (DRA) methods. In addition, borehole ovality analysis using televiewer data was undertaken to assess the orientation of the maximum horizontal stress. In addition to these measurements, the literature has been reviewed and independent reviews of all work have been undertaken. The outcomes from the various methods do not always agree and the interpretation of the stress field in a complex geological environment is not straightforward and has associated uncertainties. A back analysis of these data was undertaken using a large scale 3DEC model to assess the far field stresses.

This paper focuses on the rock mass and stress field model components of geotechnical model for the underground studies. The process used in developing these components will be discussed and the results summarised.

## 1 INTRODUCTION

The Debswana Diamond Company (DDC) Jwaneng Mine in Botswana, is a large open pit diamond mine extracting three kimberlite pipes. Open pit operations will cease in the early 2030s; studies are currently underway to transition to an underground mining operation by the time open pit mining ceases; this is known as the Jwaneng Underground Project (JUP). It is anticipated that underground mining will be undertaken using a combination of sublevel retreat (SLR), sublevel caving (SLC) and block caving (BC) methods. Mining will extend to a depth of ~1000 m below surface and will include excavations within competent country rock and weak kimberlite rock.

The JUP is currently in the prefeasibility study stage. The Exploration Access (EA) component was fast tracked, and a feasibility study completed in late 2023; mine development commenced in May 2024. The EA will provide early access for future mining as well as providing access for additional resource drilling for the deeper extents of the Kimberlites pipes.

The geotechnical model and its components are the foundation on which geotechnical design is based at Jwaneng Mine. The Jwaneng Mine has a long history of ongoing development of a high-quality geotechnical model to support open pit slope designs. This model has been updated and enhanced to support the underground studies.

## 2 JWANENG MINE SETTING

### *2.1 Location*

Jwaneng Mine is situated approximately 160 km southwest of the capital city of Gaborone in the eastern part of the Kalahari Desert. It was discovered in the Naledi Valley, southern Botswana, in 1972. In July 1982, the mine went into production and became fully operational in August of the same year (Gabanakgosi et al., 2018).

#### 2.1.1 Geology

The Jwaneng Mine country rock stratigraphy comprises Paleoproterozoic sedimentary rocks of the Pretoria Group within the Transvaal Supergroup. The upper-most stratigraphic units are the aeolian Kalahari Sands, as well as pedogenic calcretes. These units are underlain by various formations, comprising of a complex assemblage or mixture of laminated shales, quartzitic shales, and siltstones.

Below these are carbonates (dolomites) of the Malmani Subgroup West (Beukes, 2006). The simplified stratigraphy is shown in Table 1 and the country rock geology is further described in by Dunn et al. (2022a). Various dolerite (DOLR) sills and dykes are also present.

**Table 1 Jwaneng Mine Country Rock Stratigraphic Column (after Dunn et al., 2022)**

| Stratigraphic Name | Rock Type (Code) | Typical Thickness (m) |
|---|---|---|
| Kalahari Sequence | Sand & Calcrete | 55-60 |
| Timeball Hill Formation | Laminated Shale (LS) | 80 |
| Lower Timeball Hill Formation | Carbonaceous Shale (CS) | 60 |
| Rooihoogte Formation | Quartzitic Shale (QS) | Up to 600 |
| Chert Pebble Conglomerate | Bevets (BVT) | 1 - 4 |
| Rooihoogte Formation | Quartzitic Shale (QS) | |
| Lower Rooihoogte Formation | Carbonaceous Shale (CS2) | 10 |
| Malmani Subgroup | Dolomite (DM) | >700 |

Jwaneng Mine exploits a diamond-bearing kimberlite complex of three main pipes (Figure 1); these pipes have been named South (S), Centre (C) and North (N) pipes. The three pipes are associated with steep (~80°) and relatively smooth sides. The contacts with the country rock are typically very sharp. Before the onset of mining, the upper portions of the pipes were dominated by reworked volcaniclastic sediments with shallow dipping bedding structures. This is underlain by the main pipe infill which is typically dominated by broadly massive volcaniclastic kimberlite (with bedded pyroclastic and volcaniclastic units preserved in the North Pipe); there are also a range of breccias.

The main north pipe facies within the underground horizon are the VK(N) volcaniclastic kimberlite and the PK(N) pyroclastic kimberlite facies. The south pipe consists of a volcaniclastic kimberlite (VK(S)) and the AVK(S) an autolithic volcaniclastic kimberlite facies.

The centre pipe comprises of the VK(C) volcaniclastic kimberlite and three breccia units which represent zones of relatively little kimberlitic material. The CRBQS(C) and CRBDM(C) are country rock breccia units dominated by QS and DM respectively. Kimberlitic material content in these units is generally less than 5%. The KBWDM(C) unit comprises of DM clasts in relatively more kimberlitic material than the other breccias (5 – 50%).

A key challenge with these breccia units is how to characterise their geomechanical properties due to the sharp contrast in strength between the strong country rock units (QS and DM) and the weak Kimberlite material.

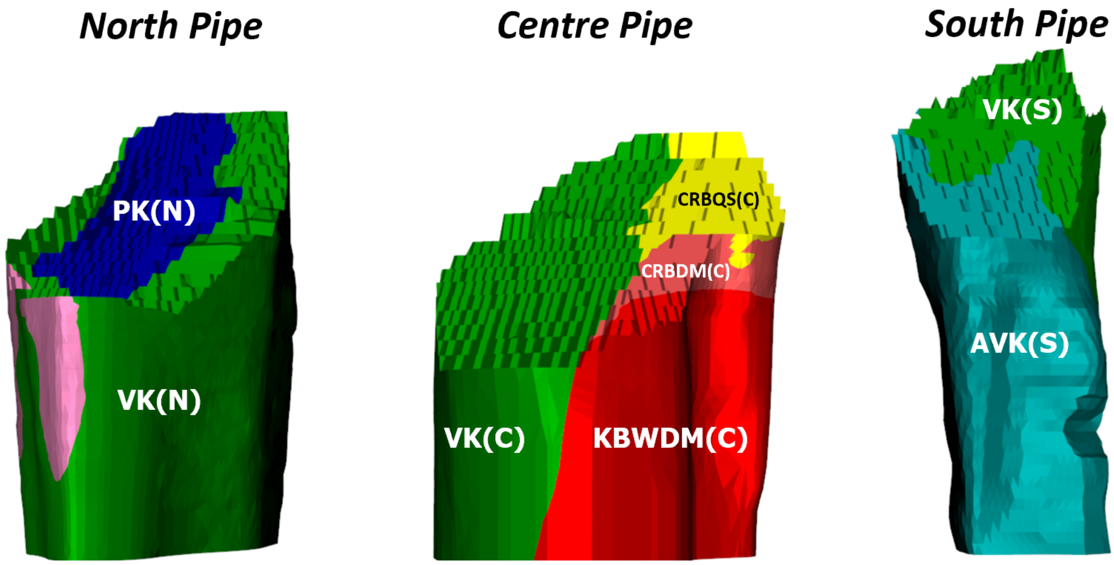


**Figure 1 Main kimberlite facies within the underground horizon (Chiwaye, 2021).**

### *2.2 Structural Setting*

The Jwaneng Mine structural setting is complex, and the structural model is updated as new information becomes available. Jwaneng Mine is dominated by NE-SW striking faults with a strong normal dip slip shear sense component. These faults are downthrown to the SE and compartmentalize the shallow to intermediately NW dipping strata into structural domains each with a unique rock fabric (Barnett, 2009). It has been suggested (Creues et al., 2017) that there have been at least three deformational events.

## 3 AVAILABLE DATA

The Jwaneng Mine geotechnical borehole database consists of approximately 529 diamond drilled boreholes with geotechnical data, from various drilling campaigns (Figure 2). These boreholes represent a cumulative length of ~226,000 m of geotechnically logged core (Kebatsetse, 2024). Most of these data are for the QS and DM; in which underground development is predominantly located.

Boreholes have been drilled in different orientations to reduce directional bias. In addition to the comprehensive geotechnical logging database, a significant amount of laboratory testing has been undertaken for a range of geomechanical tests. The database is supplemented by geophysical methods and face mapping in the open pit (Dunn et al., 2022).

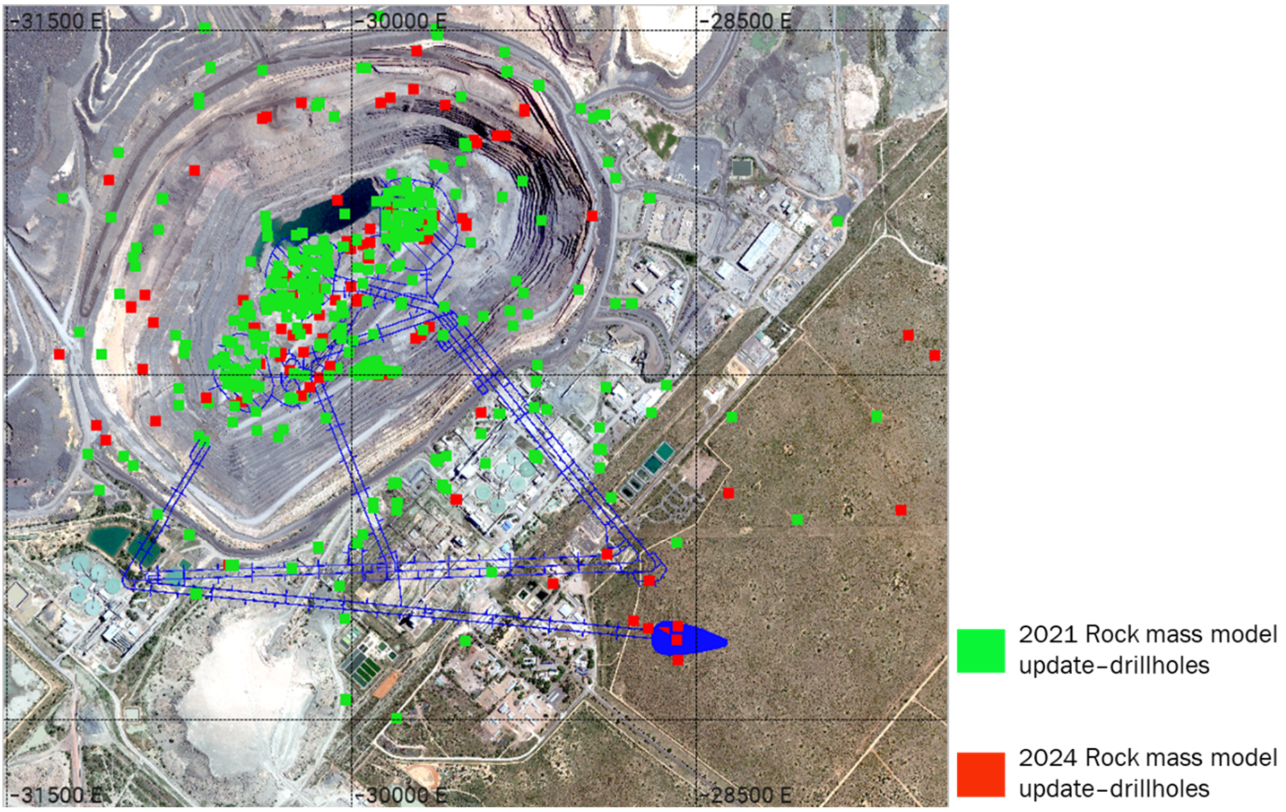


**Figure 2 Jwaneng Mine geotechnically logged drillholes and EA design (Kebatsetse, 2024).**

## 4 GEOTECHNICAL MODEL

The geotechnical model at Jwaneng Mine comprises several separate models as shown in Figure 3. The geotechnical model is regularly reviewed and updated as new data becomes available and understanding of the geotechnical environment evolves. Some investigations are carried out as part of the ongoing open pit operations while others are conducted specifically for the underground mining studies. Ultimately all learnings, regardless of where the investigations are conducted from, are consolidated into the official geotechnical model. As the stress field is an important consideration in underground mine design, it has been included in the geotechnical model development for the underground studies.

Development of the geotechnical model is undertaken in-house and is guided by the Geotechnical Review Board (GRB); which is an important part of the Debswana technical assurance process.

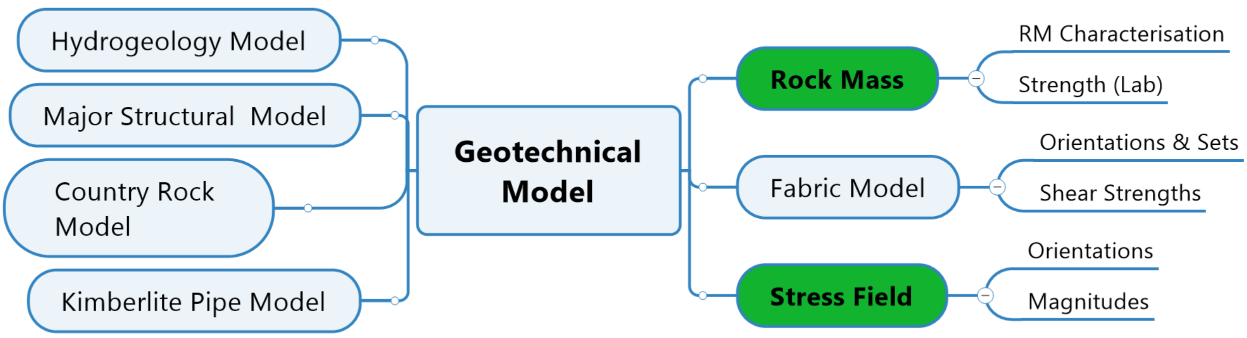


**Figure 3 Overview of geotechnical model and its components.**

### *4.1 Geology model*

The lithology model for the country rock and the kimberlites pipes is regularly updated as new drilling information becomes available; updates are typically planned to coincide with the study stages allowing for an increasing confidence level. With the changing focus to underground studies, the extent of the country rock model has been increased to consider the location of underground infrastructure, sited to the east of the open pit; this necessitated additional drilling away from the open pit.

The country rock model was updated in July 2022. A dedicated drilling programme is underway to update the Kimberlite model as part of the ongoing underground studies.

### *4.2 Structural model*

The structural model consists of two components i.e. major structures (large faults) and fabric (bedding and joints). The major structural model is regularly updated and is done when the country rock model is updated.

The fabric model is updated when the rock mass model is updated. The structural model extents have been extended to capture the access infrastructure for the underground mine.

The major structural model was updated in July 2022 (SRK, 2022). The number of faults interpreted at Jwaneng mine increased from 124 to 152 with the latest update; this is a function of additional data. The structural domains, which are blocks bounded by faults increased from 41 in 2021 to 42 structural domains in the 2022 structural model update.

### *4.3 Hydrogeological model*

The natural recharge from precipitation is limited in this semi-desert area. The water table at Jwaneng Mine is below the Kalahari sequence and hence the Kalahari Sand and Calcrete units are hydrogeologically insignificant (Itasca, 2015).

The Shale units (LS, CS and the thicker QS) are variably fractured and transmit water, though the porosity is low. Generally, the groundwater flow in the region of Jwaneng Mine is structurally controlled.

There is a network of piezometers across the site and an ongoing process of collecting hydrogeological data. This data is fed into a three-dimensional hydrogeological numerical model which is updated in sync with the study stages (Dunn et al., 2022a).

### *4.4 Rock mass model*

A comprehensive rock mass model was developed for the open pit; this model has been extended and enhanced to support the underground mining studies. A significant update of this model was undertaken in 2021 (Dunn et al., 2022a) and has been updated in 2024 (Kebatsetse, 2024).

### *4.5 Stress field*

Understanding the in-situ stress field is a critical input into underground mine design and has a significant impact on design analyses and numerical modelling. The stress magnitudes, ratios and directions of the principal stresses influence the choice of mining method, excavation stability, stand-off distances etc.

A range of stress field assessments using different techniques with extensive independent review and interpretation have been done at Jwaneng Mine. The development of the in-situ stress field model is covered by Dunn et al. (2022b) with a summary and subsequent work covered in this paper.

## 5 DEVELOPMENT OF THE ROCK MASS MODEL

Development of the rock mass model is described in Dunn et al. (2022a) and is briefly covered in the following sections.

### *5.1 Rock mass classification*

The Laubscher (1990) rock mass rating classification ($RMR_{90}$) has been used at Jwaneng Mine for open pit slope designs requirements. Several empirical methods are used for underground mine design such as the Q-system (NGI 2015) for ground support design; the Laubscher and Jakubec (2000) system ($RMR_{2000}$) for caveability assessments. The $RMR_{90}$ and $RMR_{2000}$ systems can be converted to MRMR values for caveability assessments, through the application of the appropriate adjustments for weathering, orientation, induced stress, water and blasting.

To address underground design needs, the logging system was modified in 2018 to cater for data collection needed to use the Q (NGI 2015), $RMR_{2000}$ and $RMR_{89}$ (Bieniawski, 1989) systems, in addition to the $RMR_{90}$ system. This change in logging practices required that the pre 2018 (PreQ) and the post 2018 (PostQ) data sets be evaluated to assess if they were compatible and could be combined.

Various checks were undertaken to ensure that the two data sets were comparable and could be combined (Dunn et al., 2022a). These checks focused on the joint properties where the most significant logging changes had been made.

Comparisons were made using box and whisker plots, histograms and cumulative curves and these checks confirmed that differences were negligible and that the two data sets could be combined. It is possible to extract either data set from the database if required.

Tools were developed to allow all logging parameters to be summarised using descriptive length weighted statistics, box and whisker plots, histograms and cumulative curves. This allows for analysis by rock type, spatial volumes (domains, contact zone) etc.

This approach allows the study team to better understand the data variability and assess the data confidence level. A summary of rock mass classification indices for the main rock types is shown in Table 2.

**Table 2 Rock mass classification indices for Jwaneng rock types (Kebatsetse, 2024)**

| Rock Type | Cumulative Length (m) | $RMR_{90}$ | $RMR_{89}$ | $RMR_{2000}$ | $GSI_{SRK}$ | $GSI_{Hoek}$ | Q' | Rock Mass Class |
|---|---|---|---|---|---|---|---|---|
| CALC | 6,536 | 71 | 77 | 70 | 79 | 75 | 42.0 | Good |
| LS | 7,672 | 44 | 63 | 46 | 46 | 60 | 2.6 | Poor - Fair |
| CS | 6,862 | 48 | 67 | 50 | 51 | 67 | 3.5 | Poor - Fair |
| QS | 85,404 | 54 | 72 | 57 | 56 | 71 | 4.8 | Fair |
| CS2 | 1,779 | 66 | 80 | 68 | 66 | 80 | 17.3 | Good |
| DM | 29,796 | 71 | 83 | 73 | 71 | 82 | 20.7 | Good |
| DOLR | 10,664 | 56 | 74 | 57 | 53 | 72 | 7.8 | Fair |
| VK(C) | 17,022 | 64 | 73 | 58 | 74 | 72 | 7.1 | Fair-Good |
| VK(N) | 6,253 | 63 | 69 | 54 | 73 | 66 | 4.0 | Fair-Good |
| VK(S) | 12,302 | 64 | 73 | 58 | 74 | 72 | 6.1 | Fair-Good |
| PK(N) | 12,947 | 65 | 73 | 61 | 74 | 72 | 7.5 | Fair-Good |
| AVK(S) | 1,138 | 66 | 75 | 62 | 75 | 76 | 14.4 | Good |
| CRBDM(C) | 933 | 73 | 81 | 71 | 74 | 80 | 25.7 | Good |
| CRBQS(C) | 1,105 | 42 | 64 | 53 | 43 | 59 | 15.5 | Good |
| KBWDM(C) | 1,894 | 64 | 78 | 65 | 69 | 79 | 21.4 | Good |

Two different approaches were used to calculate the GSI from core logging data: a method developed by SRK Consulting ($GSI_{SRK}$), and the method proposed by Hoek et al. (2013) ($GSI_{Hoek}$). The $GSI_{SRK}$ estimation is based on the use of the $RMR_{90}$ fracture frequency (FFr) and joint condition (JCr) ratings, each with a maximum of 40 points (Contreras, 2012).

This a is a variation on the Hoek et al. (2013) approach which is based on RQD and the $RMR_{89}$ joint condition rating. A chart defining $GSI_{SRK}$ from structure frequency on the vertical axis and surface conditions on the horizontal axis is used (Contreras, 2012).

This approach has been applied at Jwaneng for several years. $GSI_{SRK}$ has shown better correlation with GSI values estimated from pit exposures using the standard GSI chart.

Figure 4 shows box and whisker plots for $RMR_{90}$, $RMR_{89}$, $GSI_{SRK}$ and $GSI_{Hoek}$; this is a useful way to summarise data and make comparisons (Dunn et al., 2022a).

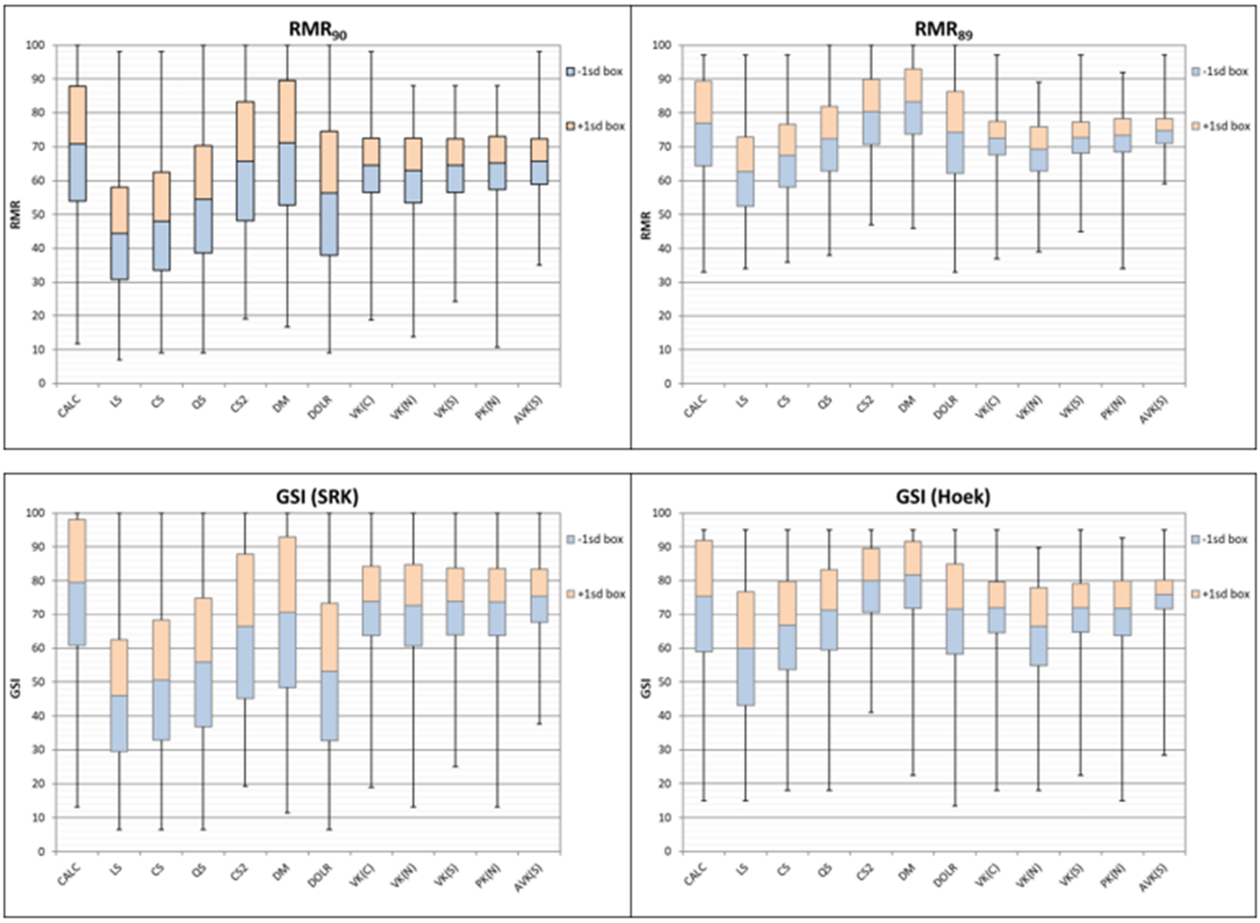


**Figure 4 Summary rock mass indices statistics at Jwaneng Mine (Kebatsetse, 2024).**

*5.2 Rock intact properties*

Jwaneng Mine has a large database of more than 13,000 laboratory tests covering a range of different test types. (uniaxial compressive strength, triaxial, tensile strength etc.). All test results are validated by the geotechnical engineers to identify valid tests and outliers.

Results are maintained in a LogChief database. Summary statistics and histograms have been developed for the each of the main rock types. Only UCS data is included in this paper as an example.

Table 3 and Figure 5 summarise the UCS for the major rock units; histograms and cumulative curves are also used. The CALC, LS and CS rock types have a moderate strength, and the QS, CS2, DM and DOLR rock types are high strength and the volcaniclastic units are low strength.

**Table 3 Descriptive statistics for UCS (Kebatsetse, 2024)**

| Stats | CALC | LS | CS | QS | CS2 | DM | DOLR | VK (C) | VK (N) | VK (S) | PK (N) | AVK (S) |
|---|---|---|---|---|---|---|---|---|---|---|---|---|
| Count | 29 | 43 | 80 | 148 | 18 | 262 | 60 | 628 | 115 | 240 | 413 | 29 |
| Mean | 74 | 48 | 119 | 232 | 309 | 250 | 266 | 31 | 40 | 26 | 59 | 28 |
| SD | 52 | 31 | 62 | 51 | 73 | 69 | 124 | 10 | 17 | 7 | 25 | 9 |
| Min | 12 | 7 | 13 | 14 | 189 | 60 | 46 | 8 | 12 | 9 | 11 | 9 |
| Max | 198 | 122 | 272 | 352 | 449 | 411 | 514 | 105 | 84 | 55 | 128 | 51 |
| COV | 70% | 64% | 52% | 22% | 24% | 28% | 47% | 33% | 41% | 26% | 42% | 32% |

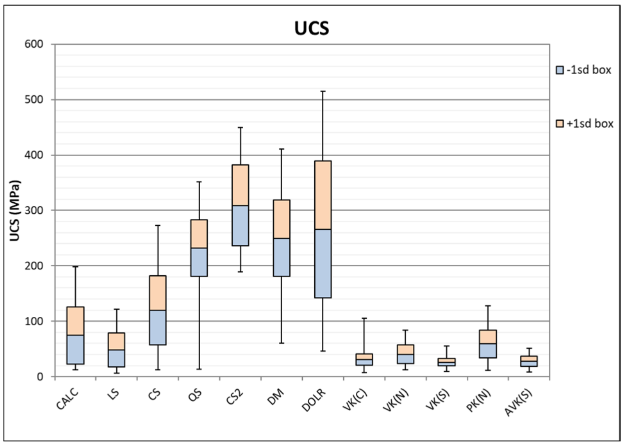


**Figure 5 Box and whisker summary of UCS results (Kebatsetse, 2024).**

*5.3 Rock mass fabric*

The rock fabric at Jwaneng varies between structural domains; therefore, the rock fabric analysis was carried out per lithology and structural domain. Data included borehole televiewer, oriented core, and face mapping datasets. Televiewer and oriented core data sets were analysed separately and showed no significant differences (Chiwaye, 2022).

Stereonets for the different structural domains analysed show similar rock fabric patterns. Generally, 3 discontinuity sets are observed (2 joint sets and one bedding set). Figure 6 shows these sets for DM rock fabric data for all blocks combined.

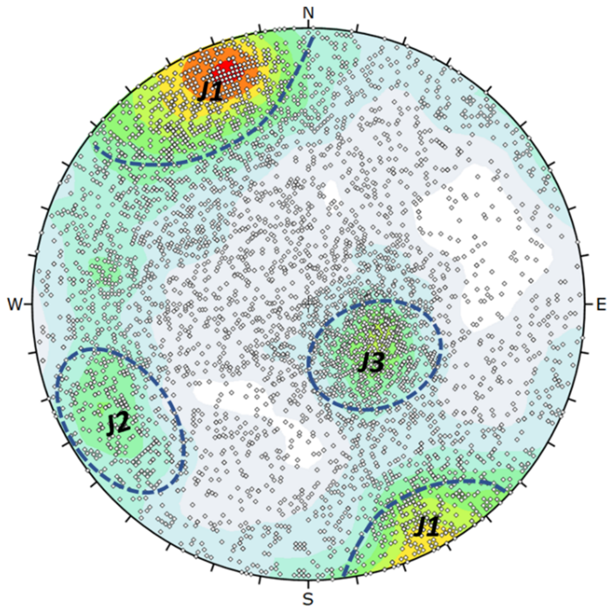


**Figure 6 Stereonet of QS and DM discontinuities (Chiwaye, 2022).**

In general, the following observations are true for the QS and DM rock fabric (Chiwaye, 2022):

- J1 is a joint set trending ENE-WSW i.e. parallel to the major fault system at Jwaneng mine. The set is steeply dipping (80 – 90 degrees) and is well developed all structural domains.
- J2 is almost orthogonal to the J1 set and has a NNW-SSE trend and is steeply dipping (70 – 80 degrees). The J2 set is poorly developed in some structural domains.

- J3 is the bedding set with shallow dips typically between 10 – 30 degrees to the NW. The bedding set is well developed and is the dominant set.
- J4 is an occasional shallow dipping set that appears in a few structural domains. This set is most likely due to localised folding of bedding planes.

The structural sets show some variations between structural domains, but the general pattern is consistent. The Jwaneng rock fabric system is characterised by 2 sets of steeply dipping orthogonal joint sets and a shallow dipping bedding set.

## *5.4 Specific analysis*

A range of analyses were undertaken to assess different aspects of the geotechnical model. These were done by spatially filtering data and generating descriptive statistics, box and whisker plots, histograms, and cumulative curves for areas of interest.

### 5.4.1 Fault characterisation and shear strength

Kebatsetse (2023) undertook an assessment of the logged fault characterisation; this considers the fault core, damage zones and the intervals adjacent to logged interval containing the fault. The main conclusions are as follows:

Fault widths are generally less than 0.3 m and are likely to have minimal impact on development advance. The length over which a fault may influence a tunnel is a function of the intersection angle. Since the fault intersections are thin, there seems to be limited influence on the rock mass quality adjacent to the fault.

Kebatsetse (2023) also investigated fault shear strengths; currently a single shear strength is used for major faults when doing numerical modelling. Several approaches were used to evaluate the shear strength, this included empirical estimates based on the logged properties, the Barton-Bandis methodology and an evaluation of limited shear box testing of fault cores.

This analysis indicated that there is variation in the fault shear strength properties; however the shear strength value currently used for design analysis falls withing the range and is considered conservative. This work is ongoing and will be refined as more logging and laboratory shear strength data becomes available.

### 5.4.2 Kimberlite contacts

Matshaba (2023) undertook a preliminary assessment of the ore -waste rock contacts using core logging data and photographs.

The contact rock mass quality presents as a minor downgrade to typical rock mass values in all kimberlite pipes, it is assessed to be less competent, and contacts are also noted to be water-bearing with most of them being wet. The north pipe presents the highest downgrade to the rock mass and may be the most challenging. The lower quality rock mass appears to mostly be constrained to a ~6 m zone around the contact.

It was concluded that due to the limited amount of data that more investigations are needed to collect the required data to the right level of quality for underground mining purposes. This will help further characterise and increase understanding of the ore-waste contacts. This data can be collected during the EA development and by the resource conversion drilling programme.

### 5.4.3 Durability and swelling

Several kimberlite facies at Jwaneng have a high proportion of swelling clays and are susceptible to slaking and swelling. X-ray diffraction (XRD) testing is used to determine the mineralogy of the kimberlite facies, including the smectite content (Dunn et al., 2022a).

The south pipe seems to have the highest levels of clay content followed by the centre pipe. The north pipe has the lowest clay content. Experiences from various drilling campaigns shows that the south pipe presents the greatest challenges due to the higher clay content.

Slake Durability Index and Duncan Free Swell laboratory tests are used characterise the different kimberlite facies. Field testing of the durability of the kimberlites was carried out by the site geotechnical team to confirm laboratory tests results.

The objective of the field testing was to assess whether the relatively short testing cycles in the laboratory were resulting in an overestimation of the durability (Chiwaye, 2021). A comparison between the laboratory and field testing is shown in Table 4.

Not all kimberlite facies show low durability and high susceptibility to weathering, and these can be quite variable. Work has commenced to understand this spatial variability; however, more data is needed, and this is being collected. This includes additional laboratory testing as well hyperspectral scanning.

Understanding the spatial distribution of swelling clays within the various kimberlite facies is critical for the design of tunnel spacing and ground support design as swelling and squeezing behaviour is expected. It is also important to understand at what percentage the presence of swelling clays becomes a problem.

If we understand the distribution and properties of swelling clays, it becomes possible to estimate likely deformations and to design an appropriate ground support system to control the expected deformation. In areas where significant swelling and associated squeezing are expected, heavier ground support will be needed, and this will impact development rates.

This information will also be important for planning purposes so that development schedules are realistic and provision for possible rehabilitation is also considered.

**Table 4 Durability classification for laboratory and field tests (Chiwaye 2021)**

| Kimberlite Facies | Laboratory | Field | Smectite Content |
|---|---|---|---|
| PK(N) | Medium - High | High | 3% |
| VK (N) | Medium | Low | 12% |
| VK (C) | Low | Low | 44% |
| VK (S) | Very Low - Low | - | 43% |
| AVK (S) | Very Low - Low | Very Low | - |
| KBWDM (C) | High | High | - |

### *5.5 Geotechnical domains*

Geotechnical domains are based on the major rock types, structural domains and the rock mass quality. When deriving the geotechnical domains, precedence was given to major rock type (lithology) with the most logging data (mainly QS and DM) as well as spatial proximity between structural domains (Chiwaye, 2021; Dunn et al., 2022a).

Six geotechnical domains have been identified within the country rock (Figure 7). Generally, the differences in rock mass quality between domains are in the order of 10-15 points for $RMR_{90}$ and GSI with both falling within the same rock mass class (Dunn et al., 2022a).

Most of the long-term access and underground infrastructure will be sited in Domains 1 and 2, within either QS or DM.

Within the kimberlite pipes the geotechnical domains are based on the different kimberlite facies. The strength of the different kimberlites and the proportion of swelling clays will determine the rock mass behaviour within the facies.

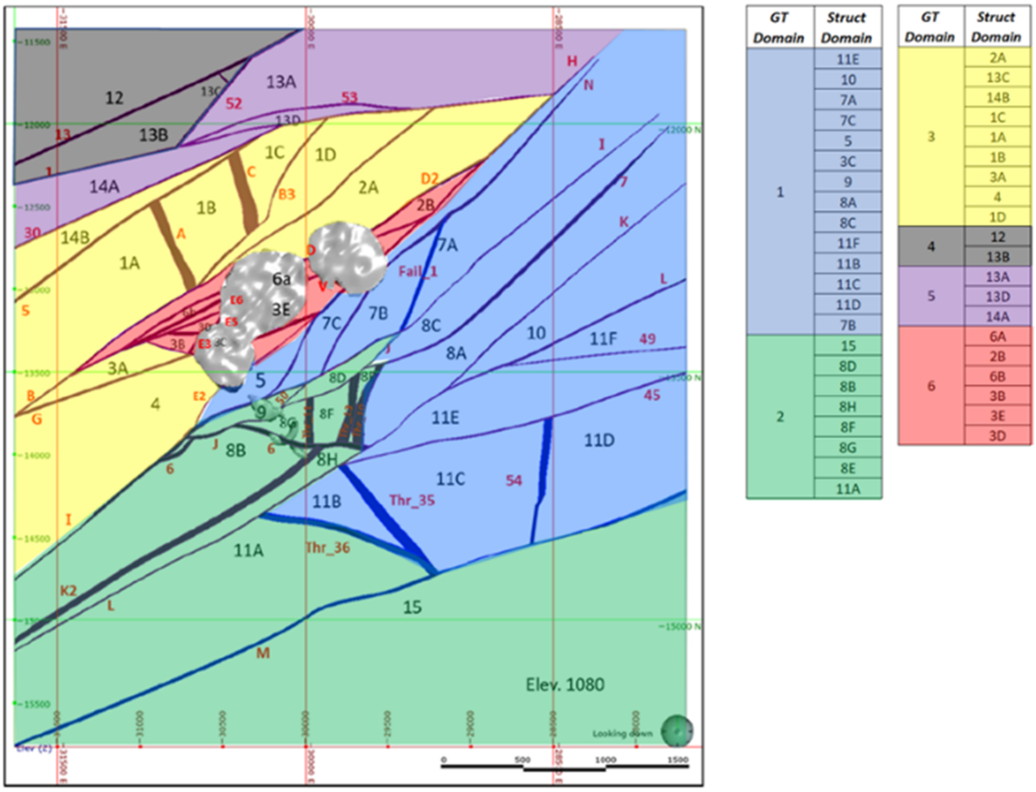


**Figure 7 Country rock geotechnical domains and structural domains (Chiwaye, 2021).**

## 6 STRESS FIELD ASSESSMENT

Significant effort has gone into assessing in-situ stress field at Jwaneng mine as detailed by Dunn et al. (2022b); a summary follows.

### *6.1 Regional stress field*

Initially, the literature was reviewed to assess the possible regional stress field; this review also considered the structural setting. From this it was inferred that the maximum horizontal stress is oriented NW-SE. Creus et al. (2017) inferred that the prevailing geological stress regime was extensional in a NW-SE direction and that Jwaneng may be at the northern most limit of a north directed compressional deformation event.

### *6.2 Stress measurements*

Several methods have been used to estimate the in-situ stress field at Jwaneng Mine as follows:

- Sigra in-situ overcore (2013) - IST
- Deformation Rate Analysis (2017) - DRA
- Sigra in-situ overcore (2019 - 2020) - IST
- Borehole Ovality Analysis (2020)
- Borehole Ovality Extended Analysis (2022)

The results are summarised and discussed in subsequent sections.

#### 6.2.1 Sigra in-situ overcore

Sigra conducted two in situ stress measurement campaigns at Jwaneng Mine using overcoring. For the first, undertaken in 2013, a total of 11 tests were attempted in 2 boreholes near the pit perimeter; five tests were deemed successful (Dunn et al., 2022b).

Results from this campaign, as re-interpreted in 2019 (Stewart & Gray, 2019) indicate the horizontal stresses are lower than the vertical stress ($S_V$) and the maximum horizontal stress is aligned NE. This is different to the regional interpretation of the maximum horizontal stress ($S_H$) orientation.

The second campaign was undertaken, drilling five boreholes remote from the open pit (Stewart et al., 2020). Twenty-four stress measurement tests were attempted, resulting in 11 successful measurements. Results indicated a horizontal stress less than the vertical stress. Two dominant maximum horizontal stress directions are present; the NW-SE trend supports the regional trend whilst the NE-SW trend is aligned with the major structure trend. The stress magnitudes and gradients for the IST measurements are summarised on Figure 8.

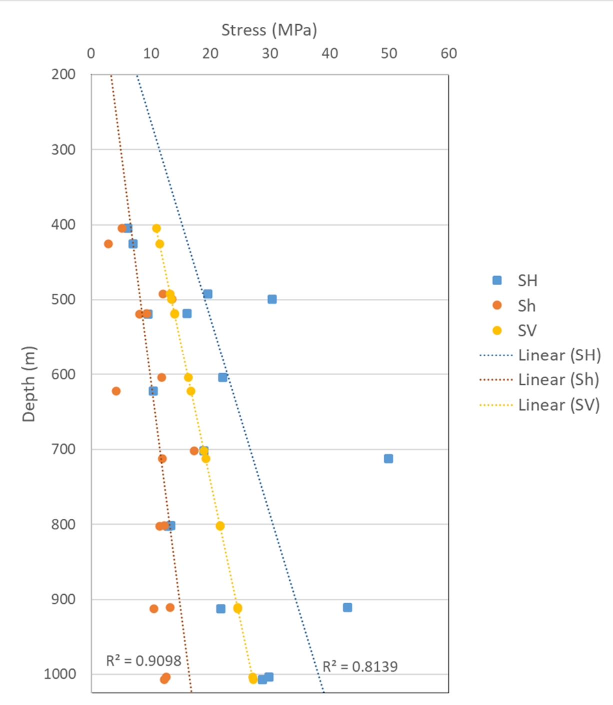


**Figure 8 IST stress magnitudes**

6.2.2 Deformation rate analysis

Five stress determinations were performed by the Australian Centre for Geomechanics (Dight & Hsieh, 2019) on core recovered from five widely distributed boreholes, using the DRA method. The principal stress orientations determined in two holes are at odds with the others and with the generally accepted orientation for Southern Africa (NNW-SSE).

Overall, the K-ratios are significantly higher than indicated by the Sigra measurements and the generally understanding of stresses in Southern Africa (Dunn et al., 2022b). The stress magnitudes and gradients for the DRA measurements are summarised on Figure 9.

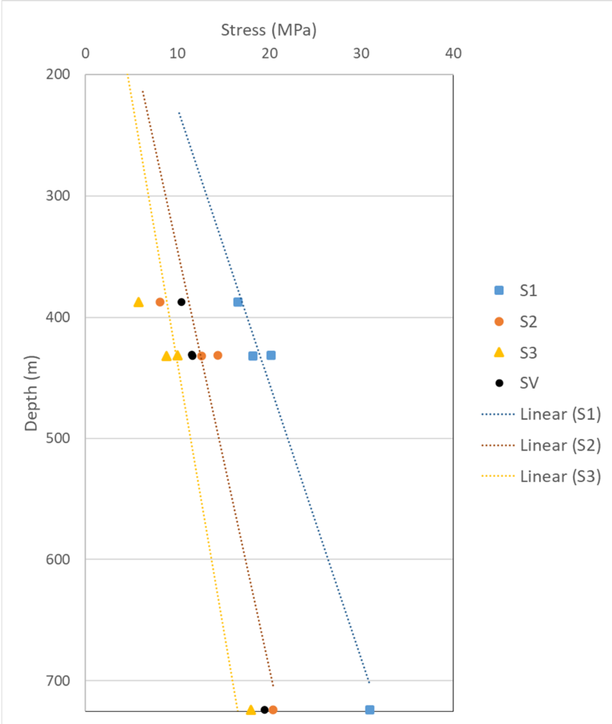


**Figure 9 DRA stress magnitudes**

6.2.3 Bore hole ovality analysis

Harvey Rock Physics (HRP) use a proprietary technique modified from breakout work performed in Aleutian back-arc, Alaska, that allows the computation of the three stress components using borehole breakout (Zajac, 1997).

In contrast, HRP modified the technique to calculate this as continuous curves denoting the orientation of the $S_H$ (maximum horizontal stress), $S_V$ (vertical stress, usually along hole) and $S_h$ (minimum horizontal stress) using borehole ovality. When the hole is vertical, SH, and Sh are in the horizontal plane; for inclined holes they are perpendicular to the hole (Dunn et al., 2022b).

Two campaigns of stress orientation analysis were undertaken by HRP, using televiewer data. The first campaign in 2020, considered 121 boreholes with teleview records; 98 of these were deemed to be useable. This analysis was focused on identifying the major horizontal ($S_H$) and minor horizontal ($S_h$) stresses; this notation must not be confused with principal stresses (Dunn et al., 2022b).

This analysis supported a NW-SE major horizontal stress orientation although there was considerable scatter, and a NE-SW orientation was also observed. This was attributed to the complex structural environment, possible open pit influences and possible measurement errors or uncertainties associated with televiewer data capture, processing and subsequent interpretation of the ovality analysis.

A second campaign of ovality analysis was undertaken in 2021 (Harvey, 2022). This was a more focused campaign, targeting the three holes used for the second Sigra (2019 – 2020) campaign so that direct comparisons could be made, as well as an additional seven holes distal from the open pit. Comparison with the Sigra data indicated that there was a good correlation in the $S_H$ orientation for 5 of the 11 measurements compared. The ovality data generally indicated a WNW to ESE orientation (Dunn et al., 2022b).

### *6.3 Interpretation and review*

Considerable variations in the data are observed and there are contradictory and conflicting results, making interpretation challenging. To assist with interpreting the results, Debswana made use of an independent GRB and technical experts. This approach has been implemented over several years and is ongoing. The outcomes of these reviews are covered in Dunn et al. (2022b); there were a range of opinions for the reviews undertaken in 2018 and early 2020, indicating considerable uncertainty.

Reviews by Mirarco (Maloney, 2020) and the GRB concluded that there was significant variation in the stress measurements and subsequently uncertainty around the stress field tensor. This necessitated the use of two stress tensor interpretations and the inclusion of sensitivity analysis in numerical modelling and design analysis. The stress field tensors are summarised in Table 5 with the vertical stress ($S_V$) assumed to be the overburden stress.

These stress tensors were used in numerical modelling analysis; however it was recognised that further work was needed; this included the second borehole ovality analysis, additional review and a numerical modelling back analysis.

**Table 5 Possible stress field tensors**

| Stress Field | $S_H$ | $S_h$ | $S_H$ Azimuth |
|---|---|---|---|
| Case 1a | 1.1x$S_V$ | 0.5x$S_V$ | 340° (NW-SW) |
| Case 1b | 0.9x$S_V$ | 0.5x$S_V$ | 215° (NE-SW) |

The stress field in the kimberlite pipes is unknown, it has been suggested that it would be lower than the country rock (Jakubec and Van As pers. comm. January 2020). Reusch et al. (2008) stated that at Panda Mine and in many volcanic pipes, the stress is lower in the pipe because of the mechanics of pipe emplacement.

### *6.4 Numerical back analysis*

Following reviews of the stress measurement results by the GRB and Mirarco (Maloney, 2020), a numerical modelling back-analysis of the in-situ stress measurements was undertaken A large-scale 3DEC model was built, incorporating major rock mass zones, orebodies, major faults as well as the pit excavation sequence. Stresses at the field measurement points were obtained from the numerical model by considering the time of field stress measurement and the corresponding pit excavation boundary.

Initial mechanical properties of rock masses and faults are assigned to the model. Then, the model input parameters of the 3DEC model are calibrated using field measured stress data at selected points. The back-analysis approach is used to calibrate the fault properties, rock mass properties and field stress parameters in the 3DEC model.

These were subsequently compared with the actual field data to determine the overall or far field representative field stress for the mine. The process is summarised in Figure 10.

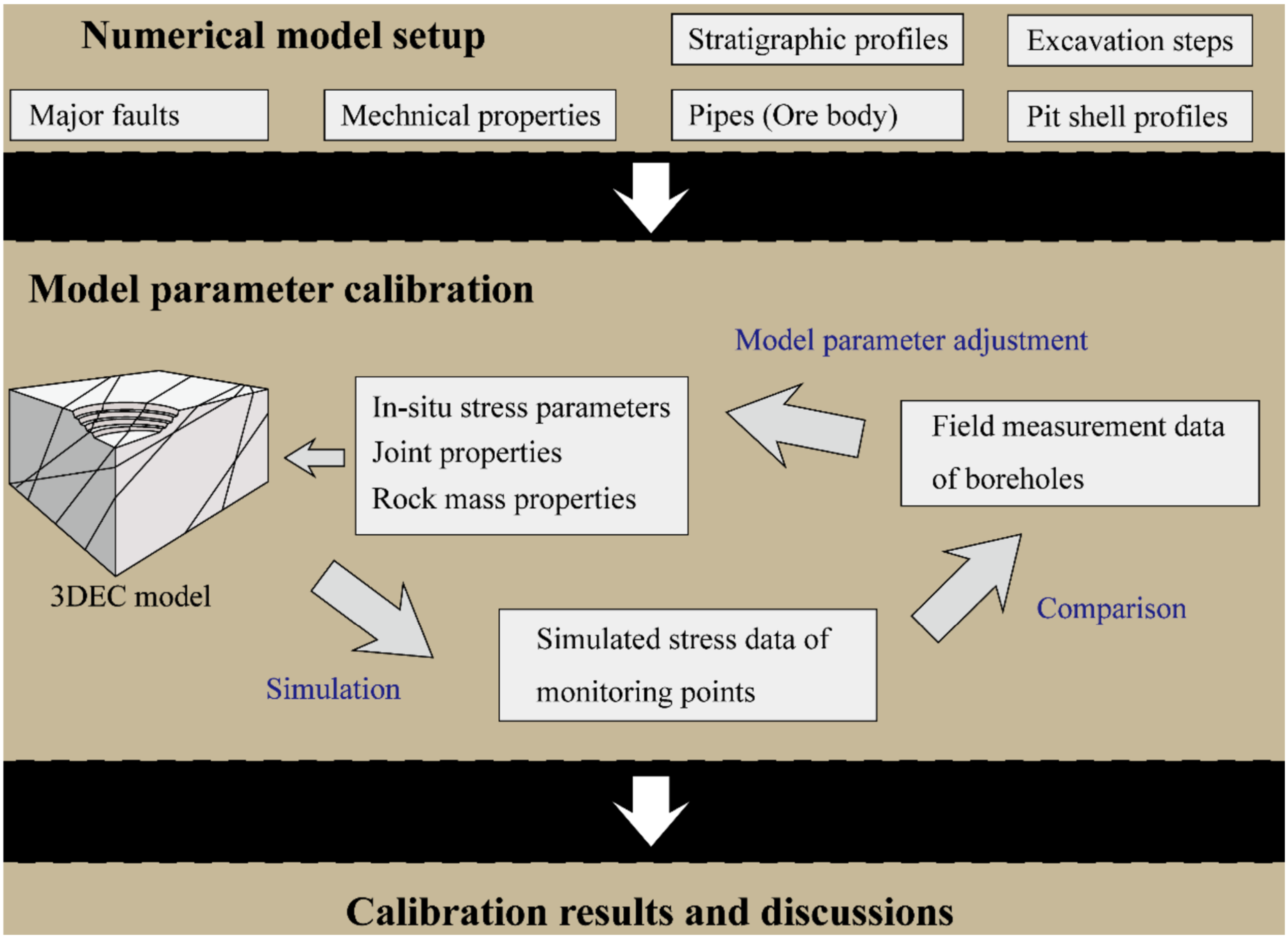


**Figure 10 Flow chart of back-analysis approach (after Mirarco, 2022)**

6.4.1 Model setup

The open pit model was constructed by starting with one large block (width 12,000 m, length 12,000 m, height 3000 m) and cutting it into smaller blocks; then, the excavation zones and rock domains are defined based on the input geometries of the pit shells and geology.

The size of the model was chosen based on the pit diameter and depth, which are about 2000 m and 800 m, respectively. The size of the model is sufficiently large so that fixed boundary conditions can be assigned to the model boundaries (Mirarco, 2022).

Faults were introduced into the model, although some simplifications were necessary. There were also simplifications terms of the geological units. Material properties were defined for the country rock and the Kimberlite pipes.

The initial field stress parameters were determined using the trend values from the field measured data (Sigra IST measurements). The initial inputs parameters such as in-situ stress parameters and mechanical properties of rock mass and faults, are further calibrated using the field stress measurement data in subsequent steps of the analysis.

Several measurement points were chosen, and the model was run with a series of excavation steps to replicate the dates when the measurements were taken. A series of monitoring points, which correspond to the stress measurement points in the boreholes, are defined in the open pit model. The simulated stresses at these monitoring points can be compared with the field measured data, and a back-analysis can be conducted to determine the representative field stress (Mirarco, 2022).

6.4.2 Back analysis method

The least-squares fitting method is used for determining the best-fit in-situ stress based on field stress measurement data. The goal is to find the optimal model parameters that best fit the field stress measurement data by minimizing the Squared Sum of Differences (SSD) of the calculated and measured stress components at each measurement point.

Firstly, the stress components for the field measurement data were transformed to the global coordinate system. Next, the offset between the numerical simulation results and the field data is evaluated. The SSD is then determined to evaluate the difference between the numerical simulation data and field measurements. The model parameters can then be adjusted according to the SSD obtained. This process is repeated several times until the minimum value of SSD is found, and the values of the model parameters defining the field stress can thus be determined.

This process is followed for each parameter whilst the other parameters are kept unchanged. Table 6 is an example of the inputs and calibration sequence. Only one parameter is calibrated in each step, and the first round is completed after all parameters are calibrated.

The parameters of interest where the K ratios ($K_H$ and $K_h$), friction angle of the major faults (Φ), Youngs Modulus (E), and the fault normal and shear stiffness (Jkn and Jks).

**Table 6 Parameter calibration sequence and initial values (Mirarco, 2022)**

| Calibration sequence | Parameter | Optimized value |
|---|---|---|
| 1 | Direction $S_H$ | 64° (TN) |
| 2 | $K_H$ ($S_H/S_V$) | 1.4 |
| 3 | $K_h$ ($S_h/S_V$) | 0.6 |
| 4 | Φ major faults | 30° |
| 5 | Jkn/Jks | 2.0 |
| 6 | Jkn | 1.0e10Pa/m |
| 7 | E (QS) | 59.6GPa |

Table 7 shows the results from the first round of optimisations for the direction of the horizontal maximum stress ($S_H$). To find the overall optimal solution, additional rounds of iterations are needed.

The parameter adjustment of the direction of $S_H$ by another two rounds of iterations is demonstrated in Figure 11. In the second round of calibration, the SSD values are reduced, indicating that the offset between simulation results and field measurement data is smaller. In the third round of calibration, the reduction of the SSD values is very small, indicating that the parameter is converging. From this it can be judged that the optimal direction of $S_H$ converges to 136.7°.

**Table 7 Results of the first round of iteration for Sigra data (Mirarco, 2022)**

| Detection sequence | Parameter | Optimized value |
|---|---|---|
| 1 | Direction $S_H$ | 132° (TN) |
| 2 | $K_H$ ($S_H/S_V$) | 1.0 |
| 3 | $K_h$ ($S_h/S_V$) | 0.6 |
| 4 | Φ major faults | 30° |
| 5 | Jkn/Jks | 2.0 |
| 6 | Jkn | 1.0e10Pa/m |
| 7 | E (QS) | 59.6GPa |

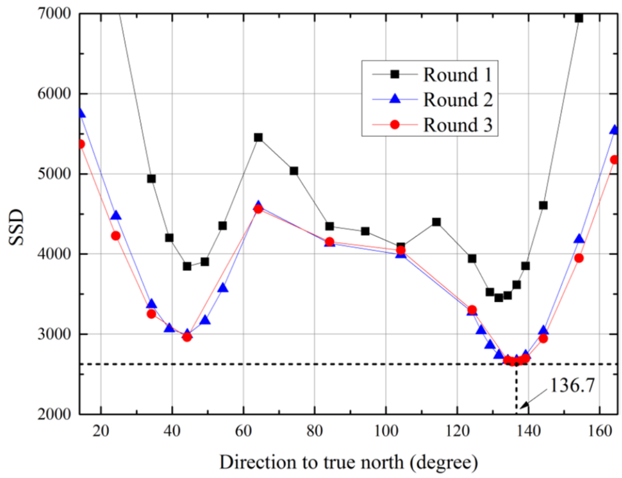


**Figure 11 Calibration of SH direction in additional rounds of iterations for Sigra data (Mirarco, 2022)**

This process was repeated for each parameter and for both the Sigra and DRA data sets.

Although the orientations of the major horizontal stress interpreted from the two datasets are close to each other, the magnitudes are somewhat different. The DRA drill holes were close to the open pit and were possibly influenced by the open pit excavation. Generally, the Sigra results were considered more reliable (Mirarco, 2022).

#### 6.4.3 Results

Table 8 shows the result from the Sigra and DRA calibrations compared with the stress fields previously used for numerical modelling at Jwaneng. The World Stress Map and Southern African stress database, indicates that $S_H$ is around 140° (NW). This agrees with the calibrated direction.

A secondary optimal solution of the direction of $S_H$ was identified, which is around 40° (i.e. NE direction). This corresponds reasonably well with the direction of Case 1b $S_H$ direction. However, the SSD value is not the overall minimum value; therefore, this secondary optimal solution was no used (Mirarco, 2022). This orientation aligns with the major fault trend and was also observed in the borehole ovality data.

The Sigra calibration was taken forward as the best solution based on current knowledge. This will be verified by underground observations and further stress measurements when there is underground access. Future measures should be taken in both the country rock and within the kimberlite pipes (Mirarco, 2022).

**Table 8 Comparison of calibration results with stress tensors previously used at Jwaneng**

| Stress Field Case | Direction of $S_H$ | $K_H$ | $K_h$ | $K_H$/ $K_h$ |
|---|---|---|---|---|
| Calibration - Sigra | 136.7° | 0.94 | 0.58 | 1.62 |
| Calibration - DRA | 139.2° | 1.5 | 0.7 | 2.14 |
| Case 1a | 160° | 1.1 | 0.5 | 2.2 |
| Case 1b | 35° | 0.9 | 0.5 | 1.8 |

## 7 DISCUSSION

### *7.1 Geotechnical model*

For the JUP the geotechnical model is the basis of the underground designs and is used to derive input properties for the rock mass and structures, as well as to define geotechnical domains. These are used in a range of analysis methods including numerical modelling.

The geology and major structures spatial models are used in numerical modelling and in various assessment whereby the proposed mine design is included in the three-dimensional model.

Updating of the geotechnical model is generally aligned with the underground study stages and is undertaken in-house. The work is guided by the internal quality assurance process in Debswana as well as by the GRB which is an important part of the Debswana technical assurance process.

### *7.2 Stress field assessment*

Understanding the stress field is critical for underground mine design where the rock stress to rock strength ratio may be unfavourable. There are a variety of ways in which stress magnitude and orientation can be assessed. In the study stages when underground access is not available, core or borehole methods are used.

For the JUP, Debswana used the IST, DRA and borehole ovality methods. Significant variations were observed between these methods making interpretation difficult. There are also difficulties associated with comparing stress measurements for different measurements methods. The DRA method produces principal stresses whilst the Sigra IST and borehole ovality methods deal with major and minor horizontal stresses and the assumption that the vertical stress is equivalent to the overburden. This complicates the interpretation and comparison of the results, specifically with respect to the magnitudes and stress ratios (Dunn et al., 2022b).

All stress measurement methods have limitations and associated uncertainties, and these can result in poor or unreliable results (Dunn et al., 2022b). There is also the influence of stress modifiers such existing excavations and geological structures such as faults, kimberlite pipes, sills and dykes.

In a complex geological environment, such as Jwaneng Mine it is difficult to avoid the possible influence of major structures, and this has likely resulted in stress rotations and the possibility of two distinct stress fields within different fault bounded structural domains (Dunn et al., 2022b).

Debswana used independent experts and the GRB to review all stress measurements and assist with the interpretation. It was decided to undertake a stress field back analysis using all the measurement data and numerical modelling. This approach resulted in a stress field estimate that agrees with the regional understanding.

When considering the various uncertainties outlined above, it is prudent to use several measurement techniques; it is also necessary to interpret all stress measurement in terms of the site structural geology and broader geological and stress setting. This is not an easy or trivial task, and the use of expert independent reviewers is beneficial (Dunn et al., 2022b).

## 8 CONCLUSIONS

This paper focuses on the ongoing development of the rock mass and stress field components of the geotechnical model. There is a significant volume of laboratory testing and geotechnical logging available at Jwaneng collected over many years. A significant amount of work has also been done in assessing the in-situ stress field.

Several parameters are logged, and these allow for characterisation of the rock mass as well as classification using a range of rock mass indices. Length weighted descriptive statistics, box and whisker plots, histograms and cumulative curves have been used to summarise and analyse data and understand the variability. Understanding the variability in the data allows for a more informed choices in design inputs.

These methods allow for comparisons between different data sets and sub-sets and are an extremely useful and powerful tool for domain analysis. Systems and processes have been developed that allow for models to be updated and analysed.

Debswana recognises that understanding the stress field is a critical input for the JUP studies. Considerable effort has gone into making stress measurements using different techniques. This has been backed up with a comprehensive literature review of the regional stress state as well as independent review to assist with interpretation. A three-dimensional numerical modelling back analysis was also done to assist in deriving the stress field inputs.

Data collection continues albeit in a more focused manner to address specific data gaps. The model components are updated to support the next study stage, and this is associated with an increasing model level of confidence. There is a well-defined quality assurance process in place to guide the development and updating of the geotechnical models.

## ACKNOWLEDGEMENT

Debswana staff who collect and process geological, hydrogeological and geotechnical data; without this contribution there can be no geotechnical model.

Various consultants who contribute to both the development of the geotechnical model and our stress field understanding.

## REFERENCES

Barnett, W. P. (2009). Jwaneng Country Rock Model Update. SRK Consulting Report.

Barnett, W. P. (2020). Dynamic 3-D Litho-Structural Model Update 2019. Jwaneng Mine, Botswana, SRK Consulting Report.

Beukes, N. J. (2006). Stratigraphy of the Transvaal Supergroup at Jwaneng Mine in Botswana, Jwaneng Phase 2 Report. KLM Consulting Services.

Bieniawski, Z. T. (1989). Engineering Rock Mass Classifications. John Wiley & Sons.

Creus, P. K., Basson, I. J., Stoch, B., Mogorosi, O., Gabanakgosi, K., Ramsden, F. & Gaegopolwe, P. (2017). Structural analysis and implicit 3D modelling of Jwaneng Mine: insights into deformation of the Transvaal Supergroup in SE Botswana. *Journal of African Earth Sciences*, vol. 137, 9–21.

Dight, P. and Hsieh, A. (2019). Jwaneng Mine in situ stress measurement report, Australian Centre for Geomechanics Report.

Chiwaye, H. T. (2021). Jwaneng Rock Mass Model Summary. Debswana Internal Report.

Chiwaye, H. T. (2022). Jwaneng Fabric Rock Mass Model Summary. Debswana Internal Report.

Contreras, L. (2012). GSI estimation from borehole data. SRK Consulting Technical Note.

Dunn, M. J., Chiwaye, H. T., Mogorosi, O. & Gabanakgosi, K. (2022a). Developing a geotechnical model for the Jwaneng underground project, in Y Potvin (ed.), Caving 2022: Proceedings of the Fifth International Conference on Block and Sublevel Caving, (pp. 109-122). Australian Centre for Geomechanics, Perth.

Dunn, M. J., Harris, R. O., Boitshepo, B. & Chiwaye, H. T. (2022b). Assessing the stress field for the Jwaneng underground project, in Y Potvin (ed.), Caving 2022: Proceedings of the Fifth International Conference on Block and Sublevel Caving, (pp. 123-138). Australian Centre for Geomechanics, Perth.

Gabanakgosi, K., Mosebi, K., Mogorosi, O., Barei, O. M., Ntlotlang, K. & Thokweng, T. (2018). A multi-disciplinary approach to dip slope mining in Jwaneng Mine, Botswana, Proceedings of the 2018 International Symposium on Slope Stability in Open Pit Mining and Civil Engineering. Seville.

Harvey, N. (2020). Stress Orientation Determination at Jwaneng Mine. HRP Consultancy Report.

Harvey, N. (2022). Stress Orientation Determination at Jwaneng Mine: Extension Study. HRP Consultancy Report.

Hoek, E., Carter, T. G., & Diederichs, M. S. (2013). Quantification of the Geological Strength Index Chart, 47th US Rock Mechanics/Geomechanics Symposium, San Francisco.

Itasca (2015). Jwaneng Mine Hydrogeology Report. Consultancy Report.

Kebatsetse, L. Q. (2023). Jwaneng Underground Project - Fault Characterisation and Classification Report. Debswana Internal Report.

Kebatsetse, L. Q. (2024). Jwaneng Geotechnical Model Update. Debswana Internal Report

Laubscher, D. H. & Jakubec, J. (2000). The MRMR Rock Mass Classification System in Mining Practice, Proceedings of MassMin 2000. Brisbane.

Laubscher, D. H. (1990). A geomechanics classification system for the rating of rock mass in mine design', The Southern African Institute of Mining and Metallurgy, vol. 90 (10), 257-273.

Maloney, S. (2020). Jwaneng Mine Early Development Project - Geotechnical Stress Measurement Assurance. Miarco Report.

Matshaba, L. (2023). Report on the Geomechanical and Hydrogeological Characterization of Jwaneng Underground Mine Ore/Waste Contacts. Debswana Internal Report.

Mirarco. (2022). Estimation of In-situ Stress Field at Jwaneng Mine. Consultancy Report.

Norwegian Geotechnical Institute (NGI). (2015). Using the Q-System – Rock mass classification and support design. Oslo.

Reusch, F., Beck, D. & Tyler, D. (2008). Quantitative forecasting of sidewall stability and dilution in Sub-level Caves', Proceedings of MassMin 2008 (pp. 453-460). Luleå University of Technology, Luleå.

SRK Consulting. (2022). Dynamic 3-D Litho-Structural Model Update 2022 - Jwaneng Mine. Consultancy Report.

Stewart, I., Smith, D., Keloth, R., Xhao, X. & Gray, I. (2020). In situ stress testing on Boreholes GT279, GT280, GT281, GT282, & GT285. Sigra Report.

Stewart, B. & Gray, I. (2019). In situ stress testing on Boreholes GT76 & GT100. Sigra Report.

Zajac, B. (1997). The State of Stress as Inferred from Deviated Boreholes: Constraints on the Tectonics of Offshore Central California and Cook Inlet, Alaska. [unpublished PhD thesis]. Caltech.